

# **A Hybrid Approach to Near-Surface Imaging and Characterization for an Onshore Niger Delta Prospect Field**

**Adizua, O. F.<sup>1,2</sup>, Anakwuba, E. K.<sup>2</sup> and Onwuemesi, A. G.<sup>2</sup>**

## **Abstract**

The imaging of the near-surface heterogeneities and its characterization finds useful applications in seismic data processing, geotechnical, civil and mining engineering projects. The conventional approaches to near-surface imaging include inversion of refracted arrivals, uphole techniques and tomography with each approach having its peculiar advantage and limitation. In this study, a hybrid and integrated approach of using both inversion of refracted arrivals and uphole measurements is presented to build a robust, more reliable and near accurate near-surface image for the prospect field being investigated. The layer properties of the near-surface (0–500 meters), was characterized in terms of weathering and sub-weathering thicknesses and seismic velocities. The near-surface model obtained was a 4-layer earth model and the seismic velocity trend observed across the layers was an increasing velocity with increasing depth trend which is commonly expected except in instances where there could be velocity inversions. The output of this study would be used in a subsequent study to derive a refraction statics solution to be used in the processing workflow for the datasets from this prospect field.

**Keywords:** Near-Surface Heterogeneities, Inversion of Refracted Arrivals, Uphole Techniques, Hybrid Approach, Seismic Velocities, Near-Surface Model

## **1 Introduction**

The near-surface is the shallow part of the earth subsurface, usually the first few tens or hundreds of meters, whose properties smear the response from deeper subsurface targets in the processing of seismic reflection data. The imaging of the near-surface heterogeneities and its characterization finds very useful applications in seismic data processing (Yilmaz, 1987; Cox, 1999 and Opara, *et. al.*, 2018) and other applications like in geotechnical investigations, civil and mining engineering projects (Gouly and Brabham, 1984; Steeples and Miller, 1990;

---

<sup>1</sup> Department of Physics (Applied Geophysics Option), Faculty of Science, University of Port Harcourt, River State, Nigeria.

<sup>2</sup> Department of Geological Sciences, Faculty of Physical Sciences, Nnamdi Azikiwe University, Awka, Anambra State, Nigeria.

Buker, *et. al.*, 1998 and Juhlin, *et. al.*, 2002). The conventional approaches to near-surface imaging include inversion of refracted arrivals, uphole survey techniques and more recently tomography. These approaches have been extensively discussed and applied in different basins around the world (Hampson and Russell, 1984; Lines and Treitel, 1984; Xianhuai, *et. al.*, 1992; Belfer and Landa, 1996; Lanz, *et. al.*, 1998; Marti, *et. al.*, 2002; Bergman, *et. al.*, 2004; Yordkayhun, *et. al.*, 2007). In the Niger Delta Basin, Opara, *et. al.*, 2018, attempted near-surface model building using refracted arrival inversion. However, the inherent limitations in relying only on refracted arrival inversion to build near-surface models, has prompted this study, in which a hybrid approach of integrating uphole measurement controls to refracted arrival inversion would be deployed to build a more reliable and near accurate near-surface earth model which could be deployed in the further processing of seismic reflection data from the area or for geotechnical, civil and/or mining engineering applications. The prospect field understudied is situated in the southern part of the Niger-Delta Basin, Nigeria. It covers areas and towns in parts of present day Rivers and Bayelsa States of Nigeria. Figure 1.0 is a map of the Niger Delta area showing the approximate location of the study area (marked in red) wherein the prospect lies.

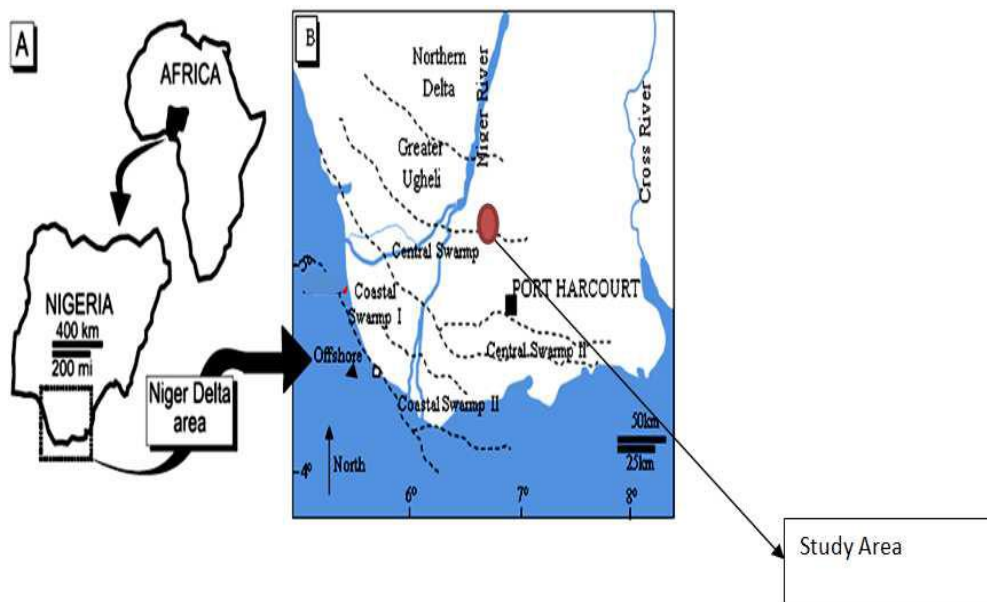


Figure 1: Map of the Niger Delta area showing location of the prospect field.

The prospect field covers an extensive area of over 151.3 square km., the geometry of the field is as shown in Figure 2.0 with its boundaries clearly defined in terms of their respective coordinates.

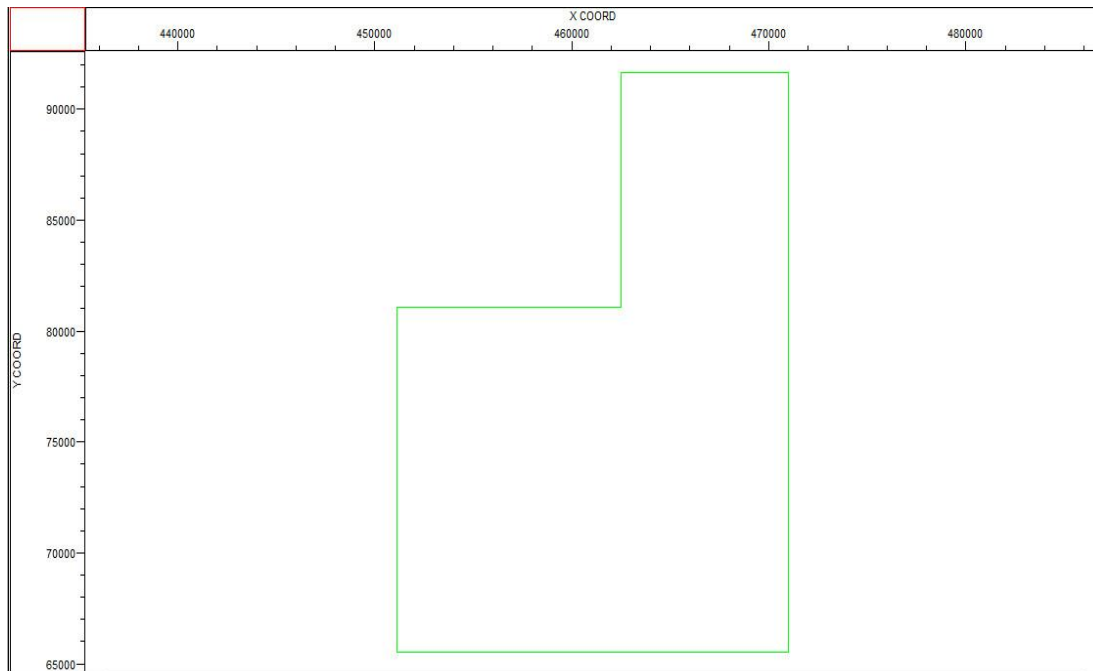


Figure 2: Geometry of the prospect field showing its boundaries and coordinates.

The terrain of the prospect is onshore but with a network of swamps, creeks and adjoining canals. The vegetation is mainly mangrove which posed a serious challenge of easy access for the seismic crew during the acquisition program. The 3D seismic acquisition for the prospect was executed in three (3) phases. Each acquisition phase covered approximately 13 swaths. The entire acquisition was done with well over 27,500 shots using a Sercel 428 recording instrument. The shooting geometry was a symmetric split spread configuration with an offset range from 25-6500m. Prior to the 3D seismic data acquisition program, a total of about 50 uphole location points were established for uphole shooting across the entire field.

## 2 Preliminary 3D Seismic Data Processing and the Near-Surface Imaging Approach

### 2.1: 3D Seismic Data and Geometry Loading, Preliminary Pre-processing and Quality Control

The acquired 3D seismic data from the prospect field were loaded using appropriate flow commands (Disk Data Input) on Promax<sup>TM</sup>. In executing the Disk Data Input flow, all the header details like trace numbers, channel numbers, field file identification (FFID) were taken into account. After the loading procedure, the raw shots acquired from the field were displayed and inspected. Figure 3.0 shows a display of the raw shots from in-line 79 in FFID and channel number order.

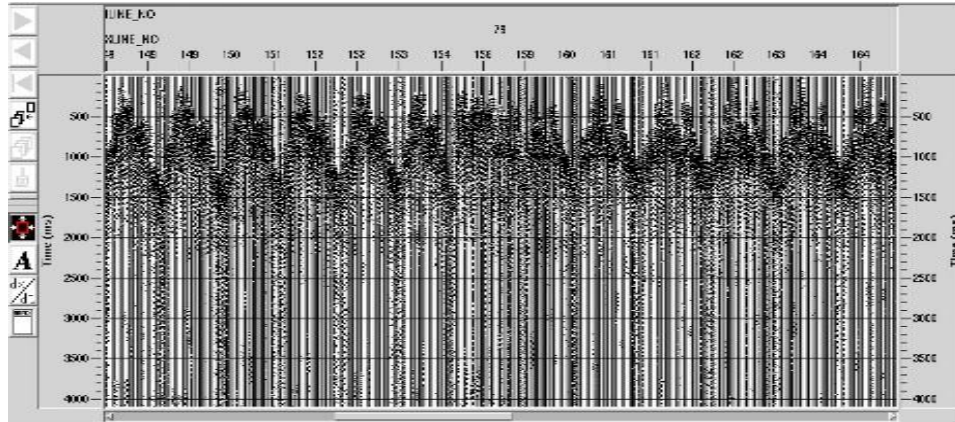


Figure 3: Display of raw shots from in-line 79 in FFID and channel number order

The geometry file for the field were equally loaded. All details that relates to receiver files, source files and relation files were all entered into a special spread sheet to load the geometry. Thereafter, QC was performed (Figure 4.0) for the loaded geometry to identify and correct possible errors associated with wrong loading of geometry. The QC check showed that geometry was properly loaded as evident from the control line (the green lines).

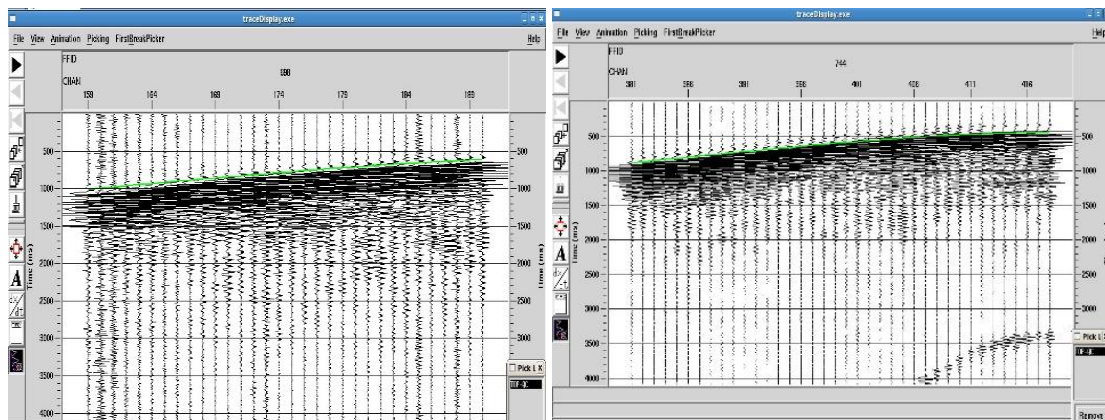


Figure 4: Quality Control (QC check) performed on loaded geometry from the field

The merging of the loaded 3D seismic data file (raw shots) and the loaded geometry (source-receiver- relation, SPS files) was subsequently performed. Linear Moveout (LMO) and LMO QC were equally performed (Figure 5.0) and preliminary frequency spectral analysis of the data to ascertain the frequency and power/energy content of the data (Figure 6.0).

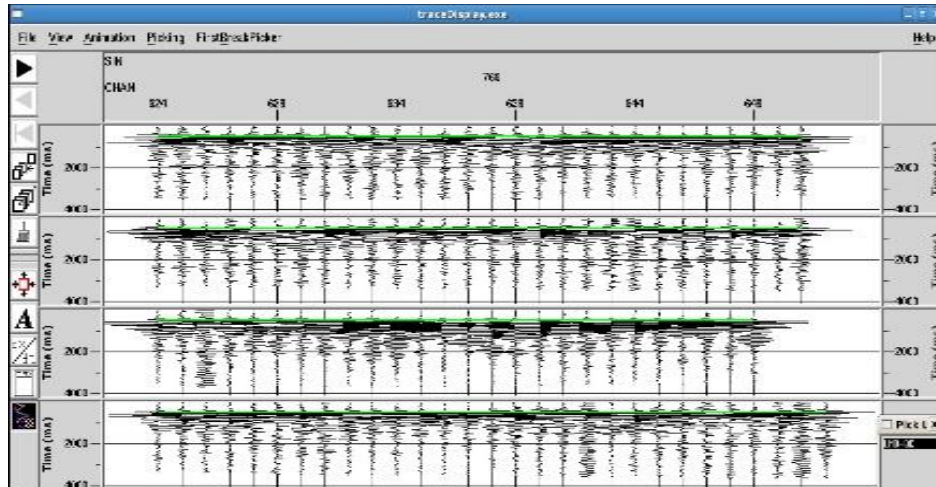


Figure 5: Linear Move out (LMO) – QC check performed was satisfactory

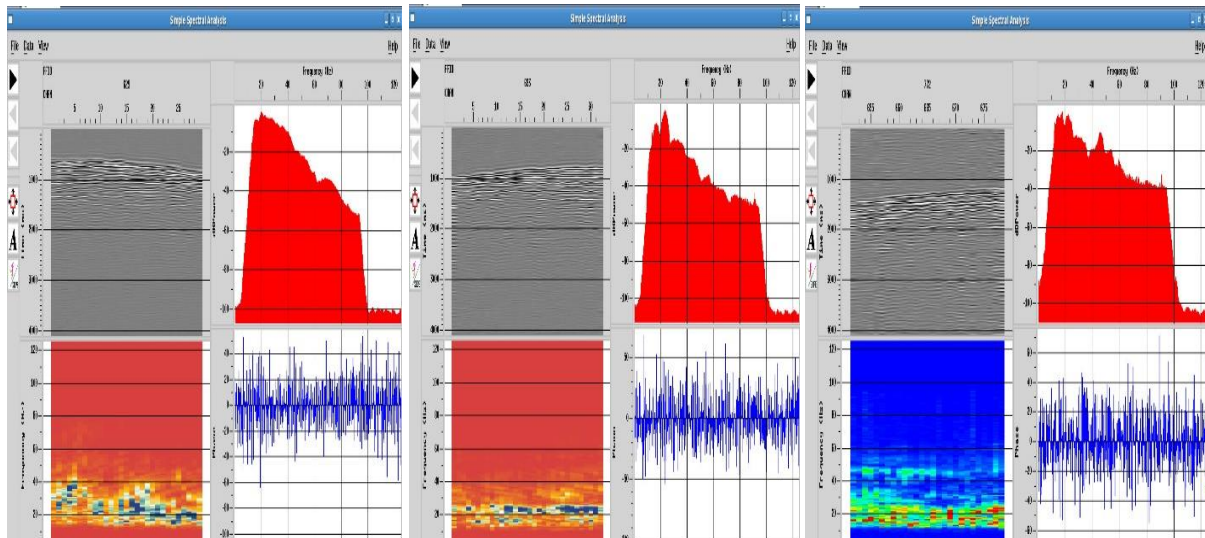


Figure 6: Frequency spectral analysis performed for different sections of the data showing the appreciable amount of energy embedded in the acquired data.

## 2.2: First Break Picking and First Break Quality Control Model for the Prospect Field

In seismic data processing, first break picking is the task of determining as accurately as possible, the onset of the first signal arrivals from a given set of seismic traces (Sabbione and Velis, 2010). Generally, these arrivals are associated with the energy of refracted waves at the base of the weathering layer or in other instances, the direct wave that travels directly from the source to the receiver. The correct determination of the onset of first arrivals (first break times) is the required and key input parameter for the inversion procedure to image or model the near-surface. The travel time of an arrival could be determined by identifying the point on the trace when the effects of the seismic wave first appear, this procedure is called picking and the end result is known as a pick, and a wiggle trace is usually the best form of display to work with. Recognizing the onset of an arrival involves identifying a change or break as it were in the character or appearance of the trace from its pre-arrival state, in terms of

amplitude, and/or frequency, and/or phase (Lankston, 1990). The picking of the first breaks for the present study was done using an automatic routine after defining appropriate time gates (time gate functions) (Figure 7.0).

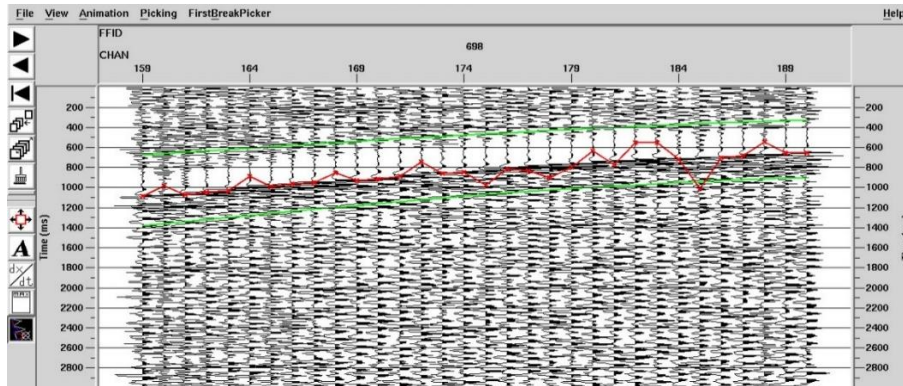


Figure 7: The automatic first break picker routine display for Channel 698. The red points are the point of picks by the routine whereas the green border lines represent the time gates defined.

The picks were later on manually edited with utmost care since time shifts due to travel time errors would ultimately lead to non-reliable models of the sub-surface (Bais *et al.*, 2003). Figure 8.0 is the edited first break pick for the channel 698 within the defined time gates.

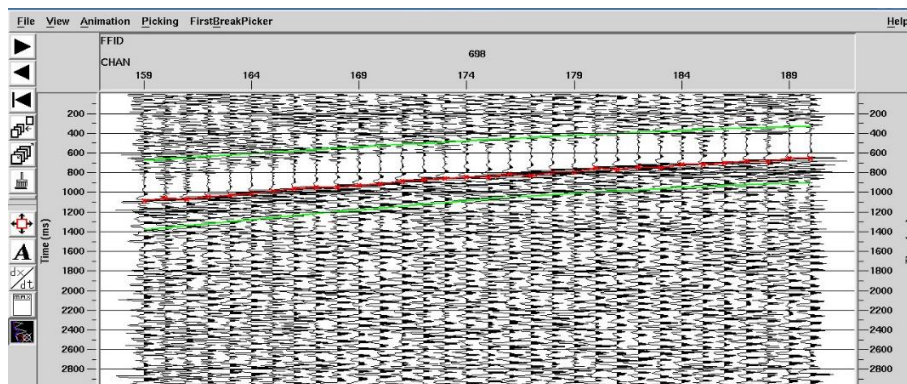


Figure 8: The edited automatic first break picker routine display for Channel 698. The red points are the point of picks, which have now been properly aligned to the onset of the first break for all the traces within this channel. The green border lines represent the time gates defined.

Standard quality control (QC) checks were performed for the picks over the prospect field (Figure 9.0), showing that the travel times were sufficiently accurate and could be inverted appropriately to yield a reliable and close to accurate near-surface model, which is the focal objective for the current study.

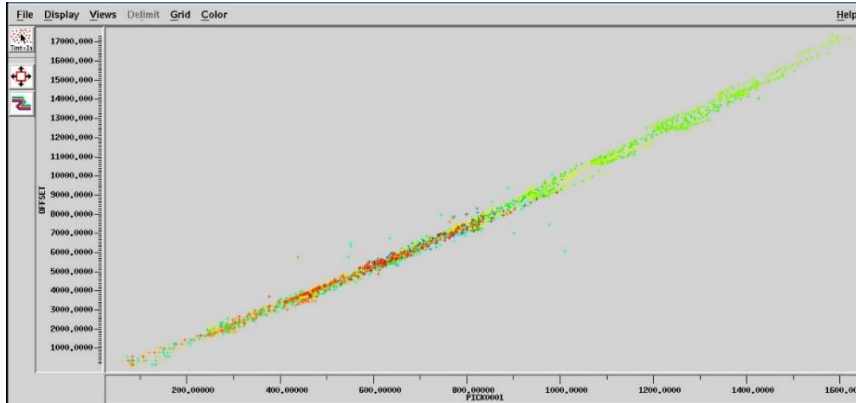


Figure 9: The first break pick QC model for the prospect. The near linear cluster of the picked points is a positive indicator that picks were accurately done and could be used as input parameter for a reliable inversion to model the near-surface.

### 2.3 Modeling Approach

The up-hole model of the near-surface, in terms of weathering and sub-weathering properties, was obtained from the up-hole survey data acquired from the prospect using the UDISYS interpretation tool and guided by the surface (shot point) correction and shot offset corrections. The refracted arrivals harvested from the 3D seismic reflection survey were equally interpreted using inverse methods. The input parameters to the inversion were the travel times of selected arrivals and the locations of the detectors and the sources. In most of the commonly used refraction data interpretation methods, it is pertinent to group arrivals that have followed equivalent paths through the sub-surface (which could be established through their ray-path trajectories). When this is achieved, the methods for inverting the travel time data is quite straightforward, but if the grouping of arrivals is inaccurate, the inversion will not produce the correct result or model which best describes the local geology. Adequate care was taken to ensure that the grouping of arrivals were accurately done. Eventually, the two near-surface models were then passed through a special in-house algorithm (program) to adaptively merge both models into an integrated and hybrid model which is more robust, reliable and a better approximation of the near-surface geology of the prospect field. The algorithm leverages on the advantages of both models to build an optimal model.

## 3 Results and Discussions

After the models obtained from both the uphole interpretation and refracted arrival inversion were integrated (merged) using the special program, four (4) major layers were identified based on their seismic velocity variations and trends; a top most weathering layer and three underlying consolidated layers. Figure 10 shows an interactive velocity picking tool bar that was used during the 1<sup>st</sup> and 2<sup>nd</sup> velocity analysis stages in the processing workflow.

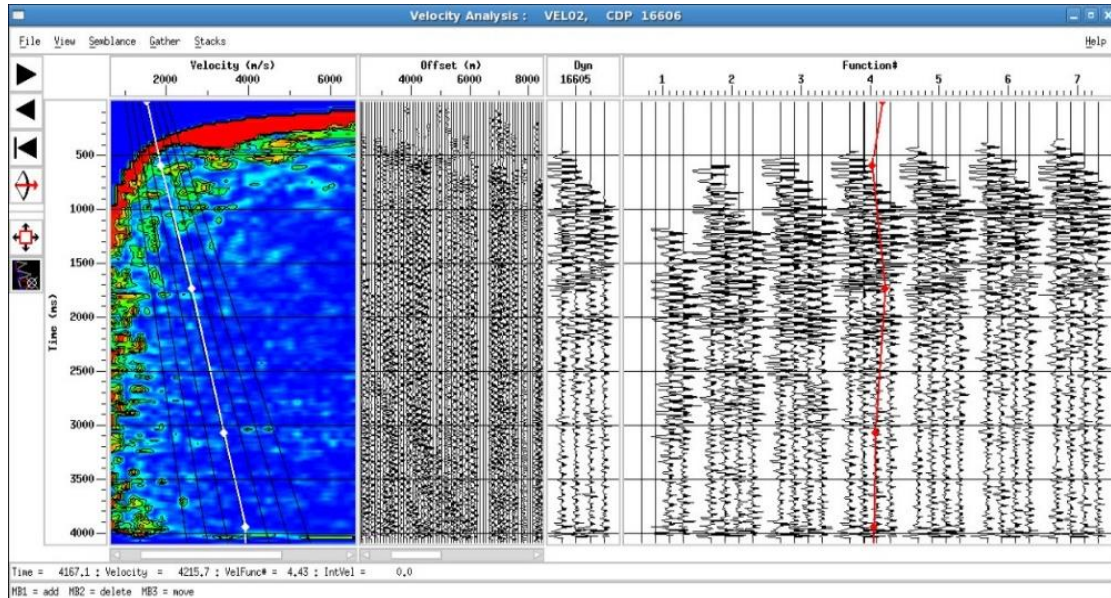


Figure 10: Velocity picking tool bar used during 1<sup>st</sup> and 2<sup>nd</sup> velocity analysis

Figure 11 and Figure 12 show the velocity field of the near-surface layers over the prospect field after the 1<sup>st</sup> and 2<sup>nd</sup> velocity analysis respectively. On close examination of both velocity fields, it is observed that there are sharp demarcations in the velocity field after the 1<sup>st</sup> velocity analysis. This sharp demarcation now blends better after slight adjustments were made to picked velocities during the 2<sup>nd</sup> velocity analysis. The velocity field (profile) after 2<sup>nd</sup> velocity analysis was taken as the optimal velocity field for the prospect.

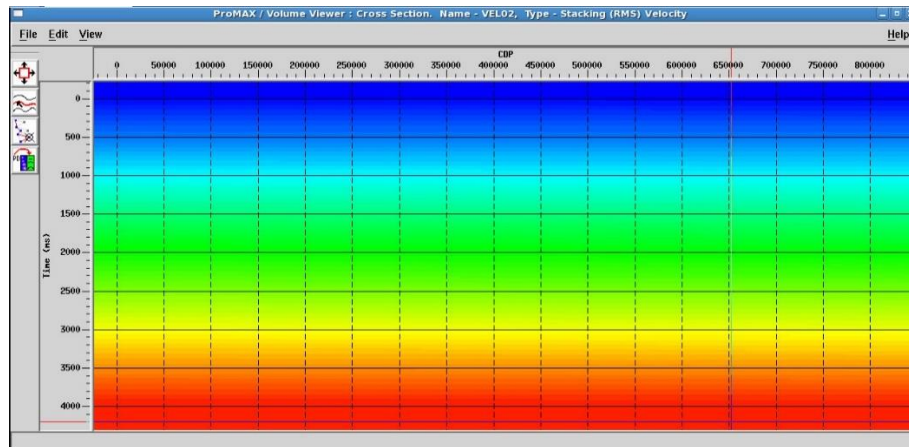


Figure 11: Velocity Field Obtained after 1<sup>st</sup> Velocity Analysis

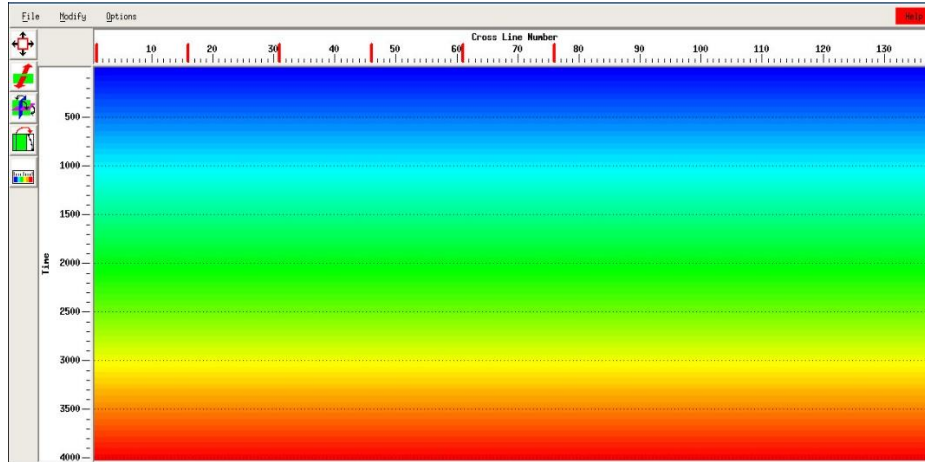


Figure 12: Velocity Field Obtained after 2<sup>nd</sup> Velocity

The obtained velocity field for the imaged near-surface layers was equally generated in In-line and X-line directions (Figure 13 and Figure 14).

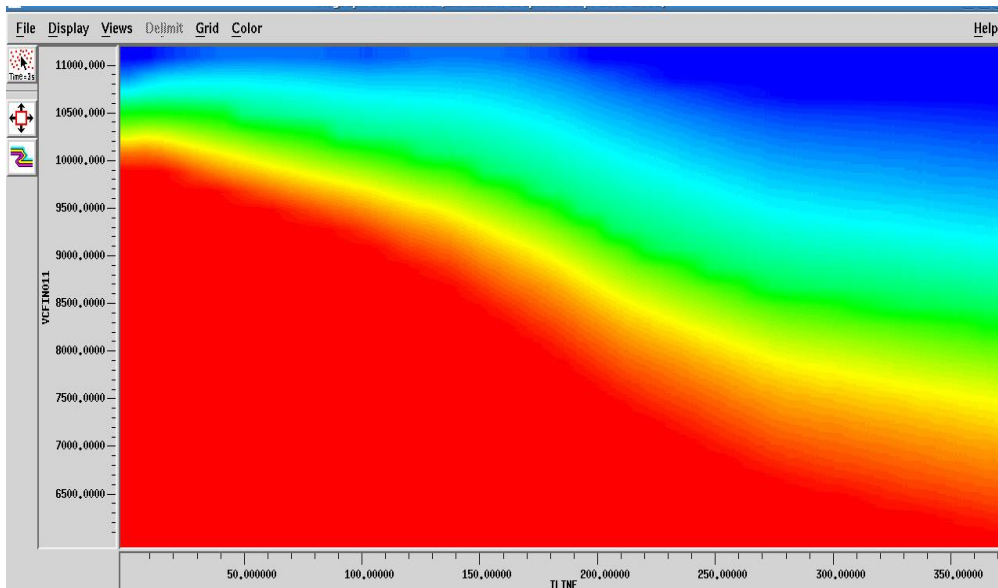


Figure 13: Velocity field in In-line Direction showing the various layers imaged

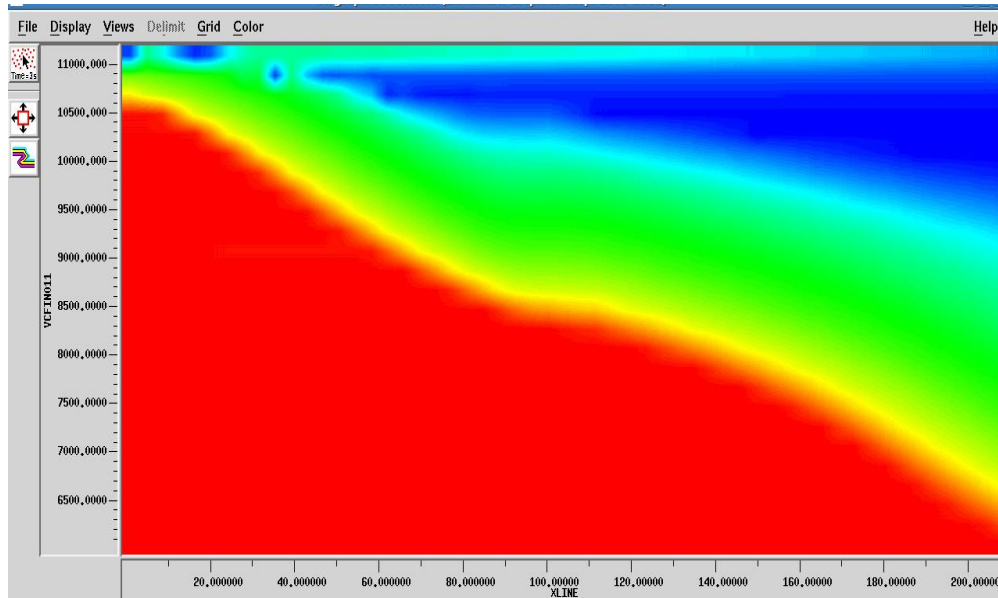


Figure 14: Velocity field in Cross-line (X-line) Direction showing the various layers imaged

The velocity trend observed in our estimation agrees with geology as velocities increased with increasing depths down the subsurface in agreement with the findings of Mares, (1984). This is an anticipated trend because increasing depths of burial would result into more compaction of sediments which would in turn increase velocities of seismic waves propagating at such zones or depths. The velocity fields over both the in-line and x-line directions are very similar. In the course of the modeling, we didn't observe any case of velocity inversions (hidden layers), where layers which should have had progressively higher velocities recorded lower velocity ranges. The in-line and x-line directions of the velocity fields were combined to create a generalized velocity field plot (Figure 15) for the prospect field.

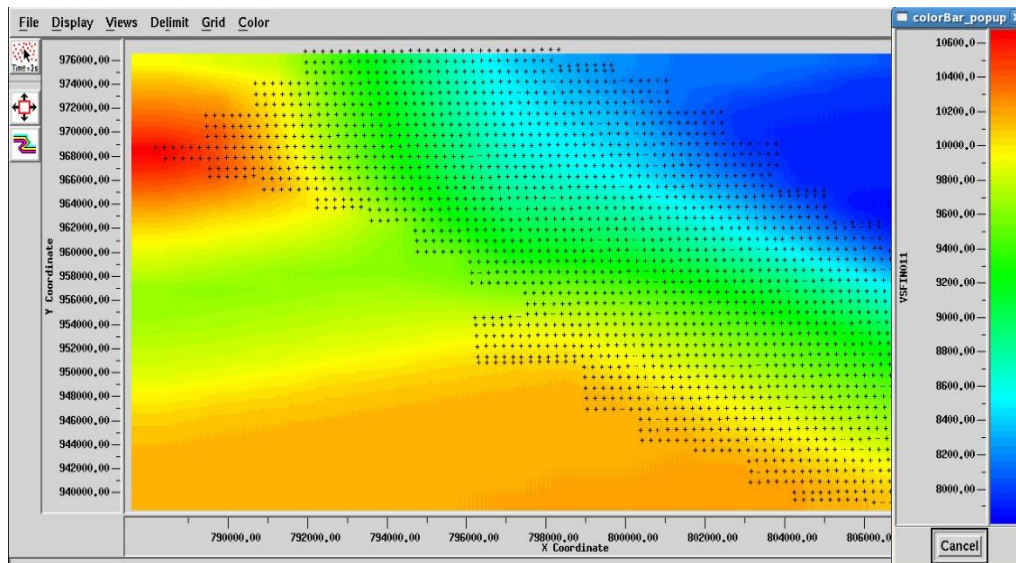
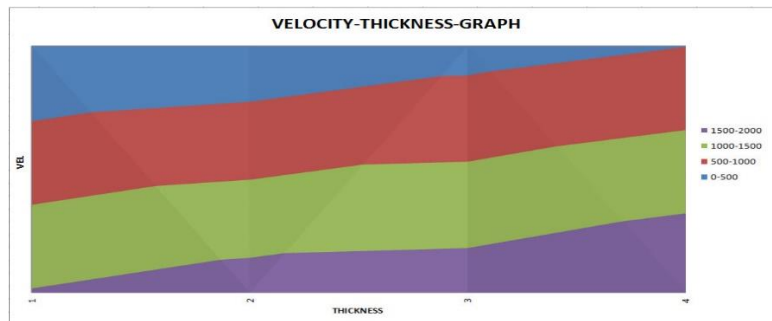


Figure 15: Generalized Velocity field over a segment of the prospect field showing the layers imaged

After successfully imaging the near-surface, the four (4) identified layers were modeled in terms of the velocity and thickness ranges in the form of a bar graph. This model is presented in Figure 15.



Bar Code	Annotation	Thickness (Depth) Range (m)	Velocity Range (m/s)
■ 0-500	Weathering Layer	3 – 18	520
■ 500-1000	First Consolidated Layer	14 – 124	1614 – 1723
■ 1000-1500	Second Consolidated Layer	62 – 322	1708 – 1758
■ 1500-2000	Third Consolidated Layer	248 – 493	1950 – 1976

Figure 15: Velocity – Thickness model with appropriate annotation

The values obtained for the weathering and sub-weathering layer thicknesses and velocities were in close proximity with values obtained from a recent literature on near-surface characterization, imaging and velocity model building within the Niger Delta Basin (Opara, *et. al.*, 2018). The velocity model of the near-surface was ideal. It increased progressively with increasing depth of burial and varied gently in the horizontal direction within the identified and imaged subsurface layers. This trend is further highlighted by a graphical

representation (Figure 16) of the thickness versus velocity trend over the prospect field and that of velocity versus thickness of imaged layers (Figure 17).

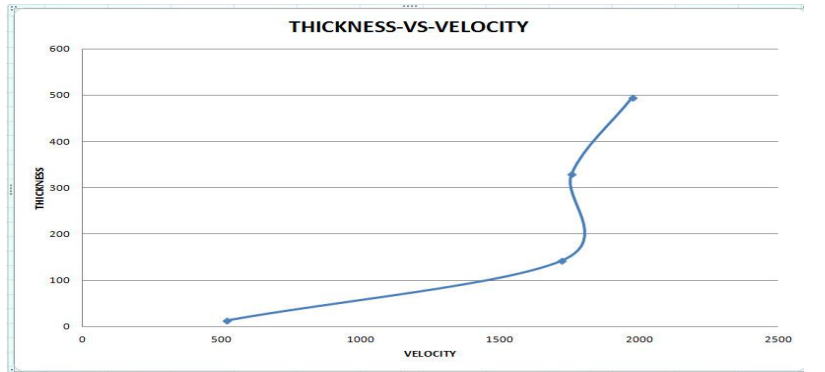


Figure 16: Thickness Versus Velocity Plot for the different layers over the prospect

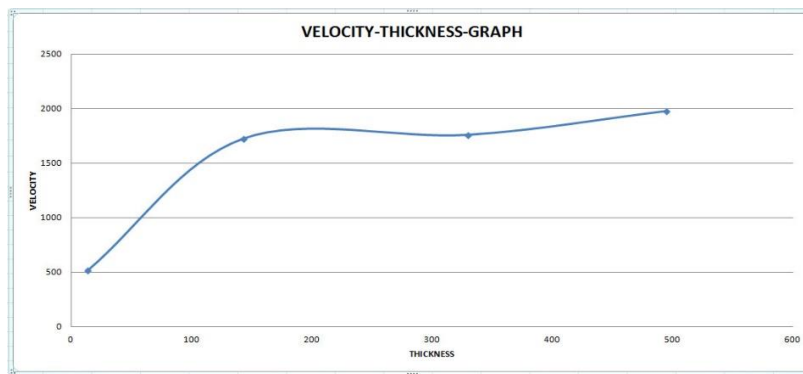


Figure 17: Velocity – Thickness graph showing mapped near-surface properties over the prospect

A block representation of the near-surface imaging and characterization results is summarized in Table 1.

Table 1: The near-surface imaging and characterization results for the prospect field.

	In-line		Cross-line	
	Velocity (m/s)	Thickness (m)	Velocity (m/s)	Thickness (m)
Weathering Layer	520	5-14	520	3-18
1 <sup>st</sup> Consolidated Layer	1614-1723	10-143	1568-1748	14-124
2 <sup>nd</sup> Consolidated	1708-1758	71-330	1736-1786	62-322
3 <sup>rd</sup> Consolidated	1950-1976	314-495	1923-1942	248-493

## 4 Conclusion

We have successfully characterized and imaged the near-surface (uppermost 500m) over the Niger Delta prospect field using a hybrid and integrated approach of combining both refracted arrival inversion and uphole survey interpretation/modeling approaches. The near-surface model comprised of a weathering layer whose thickness ranged from 3-18m and whose seismic velocity was approximately 520m/s. Three sub-weathering layers were equally imaged, with their respective thicknesses and seismic velocities also obtained. It was observed from the range of velocities obtained for the various layers, that velocities increased progressively as depths imaged increased in both in-line and cross-line directions across the field. This is an expected trend except in situations where velocity inversions occur. We equally observed that along imaged layers, velocity values varied gently across the individual layers with no incidences of sharp velocity variations or contrast within an imaged layer. The output of this study will serve as an invaluable guide for geotechnical, civil and mining engineering applications or for implementing a refraction statics solution for the further processing of the 3D seismic dataset, which would form the basis for a new study.

### Acknowledgement

Our industry partners, who wish to remain anonymous, are highly appreciated and acknowledged for providing the seismic and uphole survey datasets used for the study and for availing our team of some technical and processing facilities/supports. The University of Port Harcourt, Nigeria and the Nnamdi Azikiwe University, Nigeria are acknowledged for providing the research platforms and the enabling environment for the research to thrive. This study couldn't have been realized without the insightful contributions of some intelligent and experienced geoscientists with whom we had very meaningful discussions. They are all highly appreciated.

## References

- [1] Bais, G., Bruno, P. G., Di Fiore, V. and Rapolla, A., (2003): Characterization of shallow volcano-clastic deposits by tuning ray seismic tomography: an application to the Naples urban area. *Journal of Applied Geophysics*, Volume 52, p.11-21
- [2] Bergman, B., Tryggvason, A. and Juhlin, C., (2004): High resolution seismic travel time tomography incorporating statics corrections applied to a till-covered bed rock environment. *GEOPHYSICS*, Volume 69, p.1082-1090
- [3] Buker, F., Green, A. G. and Horstmeyer, H., (1998): Shallow seismic reflection study of a glaciated valley. *GEOPHYSICS*, Volume 63, p.1395-1407
- [4] Cox, M., (1999): Statics correction for seismic reflection surveys. Society of Exploration Geophysicists (SEG) Publication, Tulsa – Oklahoma, 531p.
- [5] Gouly, N. R. and Brabham, P. J., (1984): Seismic refraction profiling in opencast coal exploration. *First Break*, Volume 2 Issue 5, p.26-34.
- [6]

- [7] Julin, C., Palm, H., Mullern, C. and Wallberg, B., (2002): Imaging of Groundwater resources in glacial deposits using high resolution reflection seismic. Sweden Journal of Applied GEOPHYSICS, Volume 51, p.107-120
- [8] Lankston, R. W., (1990): High resolution refraction seismic data acquisition and interpretation. In Ward, S. H. (Ed), Geotechnical and Environmental Geophysics, Volume 1, Society of Exploration Geophysicists, Investigations in Geophysics Volume 5, p.45-73
- [9] Lanz, E., Maurer, H. and Green, A. G., (1998): Reflection tomography over a buried waste disposal site. GEOPHYSICS, Volume 63, p.1414-1433
- [10] Mares, S., (1984): Introduction to Applied Geophysics, Reidel D. Publishers, Dordrecht, Lancaster, 581p.
- [11] Marti, D., Carbonell, R., Tryggvason, A., Escuder, J. and Perez-Estaun, A., (2002): Mapping brittle fracture zones in three dimensions: High resolution travel time seismic tomography in a granitic pluton. Geophysical Journal International, Issue 149, p.95-105
- [12] Opara, C., Adizua, O. F. and Ebeniro, J. O., (2018): Near-surface seismic velocity model building from arrival travel times – A case study from an onshore Niger Delta field.
- [13] Universal Journal of Physics and Applications - UJPA (Horizon Publishing – HRPUB), Volume 12, Issue 1, p.1-10
- [14] Sabbione, J. I. and Velis, D., (2010): Automatic first – breaks picking: New strategies and algorithms. GEOPHYSICS, Volume 75, Number 4, p.67-76
- [15] Steeples, D. W. and Miller, R. D., (1990): Seismic reflection methods applied to engineering, environmental and groundwater problems. In: Ward, S. H. (Ed), Geotechnical and Environmental Geophysics, I: Review and Tutorial. Society of Exploration Geophysicists – SEG, p.1-30
- [16] Xianhuai, Z., David, P. S. and Burke, G. A., (1992): Tomostatics: Turning ray tomography + static corrections. Geophysics: The Leading Edge (TLE) of Exploration. p.15-23
- [17] Yilmaz, Ö., (1987): Seismic data processing, Society of Exploration Geophysicists (SEG) special processing manual, Tulsa, USA. 2027p.
- [18] Yordkayhun, S., Juhlin, C., Giese, R. and Cosma, C., (2007): Shallow velocity – depth model using first arrival travel time inversion at the CO2 SINK site, Ketzin, Germany. Journal of Applied Geophysics (ScienceDirect), Volume 63, p.68-79